Load Prediction for the Extrusion from Circular Billet to Symmetric and Asymmetric Polygons Using Linearly Converging Die Profiles

Article *in* Key Engineering Materials · September 2014

DOI: 10.4028/www.scientific.net/KEM.622-623.119

CITATIONS
2

READS
50

2 authors:

Js Ajiboye
University of Lagos
21 PUBLICATIONS **181** CITATIONS
SEE PROFILE

Sunday T. Oyinbo
University of Johannesburg
24 PUBLICATIONS **171** CITATIONS
SEE PROFILE

Key Engineering Materials Vols. 622-623 (2014) pp 119-128 *Online: 2014-09-26*
© (2014) Trans Tech Publications, Switzerland
doi:10.4028/www.scientific.net/KEM.622-623.119

Load Prediction for the Extrusion from Circular Billet to Symmetric and Asymmetric Polygons Using Linearly Converging Die Profiles

J. S. Ajiboye[1] and S. T. Oyinbo

Department of Mechanical Engineering, University of Lagos, Nigeria

[1]josyajiboye@gmail.com

Keyword: Symmetric, asymmetric, Polygons, extrusion, linearly converging dies, FEM modelling

Abstract. The deformation load is the most important parameter in the press design as it affects the structure and the general integrity of the final product. Therefore, every other parameter such as die shape, friction, type of process (hot or cold), and speed considered in modeling is optimized to cut back on the metal forming load. The flow of metal is largely influenced by the geometry of the die and hence the geometric shape of the tools is the main factor by which an optimum load can be evaluated. In extrusion process the strain distribution, resulting from deformation load, and other important variables that influence material structure, such as a hydrostatic stress, are strongly dependent on the geometry of the die. In the present investigation using linearly converging die profiles, the extrusion of symmetric and asymmetric polygons such as circular, square, triangular, hexagonal, heptagonal, octagonal, and L-, T- and H-, respectively sections from round billet have been numerically simulated. Mathematical equations describing the die profiles were derived, and then using MATLAB R2009b the co-ordinate of the die profiles was evaluated. A solid CAD model for the linearly converging die profile was made using Autodesk Inventor 2013 software and numerical analysis using DEFORM software for extrusion of the above sections from round billet was then performed to predict, for dry and lubricated condition, the extrusion load during deformation. It is found that the predictive loads for asymmetric shapes are found to be higher than that of the symmetric shapes. While there is no marked difference between the predictive loads for symmetric shapes that of the asymmetric shapes is significant where L-section has the highest extrusion load, followed by T-section and the H-section given the least pressure.

Introduction

The deformation load is the most important parameter in the press design as it affects the structure and the general integrity of the final product. The amount of metal forming load, which come from die shape and other extrusion parameters, employed in the deformation has great consequence on the strain and structure evolution [1,2,3,4]. Therefore, so many extrusion parameters have been studied in recent time so as to have smooth flow during metal forming operations to cut down on the forces involved [5]. Different die geometries such as third order polynomial equation, fifth order polynomial equation, Bezier curve, etc., have been suggested [6, 7] for the design of streamlined extrusion dies with the view to reduce the extrusion load for the given reduction ratio. They suggested extrusion dies with cosine profile to extrude circular billet to circular shape and using upper bound solution, plastic deformation work required for extrusion is determined. It has been proved that the die designed based on cosine profile is superior to the conventional shear dies and the straightly converging dies. Maity et al. [12] studied the effect of mathematically contoured die on surface integrity of extruded product. They used three dimensional upper bound methods using dual stream function method to obtain non-dimensional extrusion pressure and optimum die length for cosine die profile for different reductions. They found that the experimental results are compatible with the theory. Many analytical methods especially upper bound has played prominent role in analyzing metal forming operations. But like many other analytical methods, upper bound suffers from several limiting assumptions such as material characterization, isotropic and homogeneity of material. Consequently, numerical methods especially FEM have largely taken over in metal forming analysis [14, 15]

A major limitation to the success of any extrusion operation is the capability of the particular extrusion press to meet the maximum pressure requirements for the operation. Most plastic extrusion companies lack the equipment required to produce consistent, tight tolerances on regular and irregular polygons. Consequently, the current work seeks to provide solution through finite element modelling of extrusion dies. This will be done through careful design of the extrusion die profile to control the pressure requirement, product structure and thereby minimize the amount of inhomogeneity imparted into the product.

Die Design Profile

In the present investigation the linearly converging profiles have been designed for extrusion of circular, square, triangular, hexagonal, heptagonal, octagonal, L-, T-, and H- sections from round billet. Once the plastic extrusion design is finalized and the die is machined using Computer Aided Design and Computer Aided Machining (as required) the extrusion is done to precise specifications. Here, a mathematical equation of the die profile is derived, then using MATLAB R2009b we calculate the co-ordinate of the die profile. A solid CAD model for the linearly converging die profile is made using Autodesk Inventor 2013 software.

Geometry of die profile for extrusion of triangular (equilateral) section from round billet. The billet is of circular shape with radius R and product is of triangular shape with half width of each side is A. i. e. 2A = side of the triangle; Half side of the triangle = A; R = radius of the circular billet The distance from CG to any vertex of the triangle$=\frac{2A}{\sqrt{3}}$; P and N again represent the number of steps from extreme outer edge towards the center of the triangle as described earlier.
After (P) Steps: P<N

Focal length = a=OO'=$R-\left(R-\frac{A}{\sqrt{3}}\right)\frac{P}{N}$. That is, the coordinate of O' is $\left(R-\left(R-\left(\frac{A}{\sqrt{3}}\right)\right)\left(\frac{P}{N}\right),0\right)$. M and P has coordinate $\left(R-\left(R-\left(\frac{2A}{\sqrt{3}}\right)\right)\left(\frac{P}{N}\right)\right)\left(\frac{1}{2}\right),\left(R-\left(R-\left(\frac{2A}{\sqrt{3}}\right)\right)\left(\frac{P}{N}\right)\right)\left(\frac{\sqrt{3}}{2}\right)$ and $\left(R-\left(R-\left(\frac{2A}{\sqrt{3}}\right)\right)\left(\frac{P}{N}\right)\right)\left(\frac{1}{2}\right),-\left(R-\left(R-\left(\frac{2A}{\sqrt{3}}\right)\right)\left(\frac{P}{N}\right)\right)\left(\frac{\sqrt{3}}{2}\right)$, respectively.

The equation of the parabola passing through points with vertex at $\left\{\left(R-\left(R-\frac{A}{\sqrt{3}}\right)\left(\frac{P}{N}\right)\right),0\right\}$ is given by

$$-y^2=4\alpha\left(x-(R-(R-\frac{A}{\sqrt{3}})\left(\frac{P}{N}\right)\right) \quad (1)$$

where 4α is to be determined from the knowledge that the parabola passes through the point $\left\{\left(R-\left(R-\frac{2A}{\sqrt{3}}\right)\left(\frac{P}{N}\right)\right)\left(\frac{1}{2}\right),\left(R-\left(R-\frac{2A}{\sqrt{3}}\right)\left(\frac{P}{N}\right)\right)\left(\frac{\sqrt{3}}{2}\right)\right\}$

Putting these values of x and y in the equation (1), we get

$$-\left(R-\left(R-\frac{2A}{\sqrt{3}}\right)\left(\frac{P}{N}\right)\right)^2\left(\frac{3}{4}\right)=4\alpha\left\{\left(R-\left(R-\frac{2A}{\sqrt{3}}\right)\left(\frac{P}{N}\right)\right)\left(\frac{1}{2}\right)-\left(R-\left(R-\frac{A}{\sqrt{3}}\right)\left(\frac{P}{N}\right)\right)\right\}$$

Solving, we get

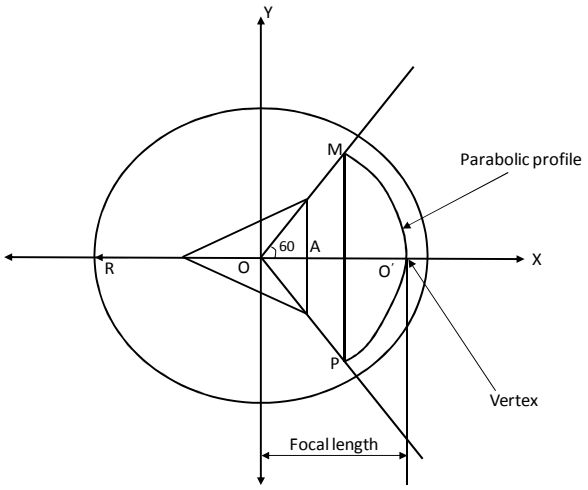

Fig. 1 The die profile (plan view) from round to triangular section

$$4\alpha = \frac{\left(\frac{3}{2}\right)\left[R-\left(1-\frac{P}{N}\right)+\left(\frac{2AP}{N\sqrt{3}}\right)\right]^2}{\left(R\left(1-\frac{P}{N}\right)\right)} \tag{2}$$

Where P = 1, 2, 3 …….. N-1

Putting the value of 4α into equation 1, the equation of the parabola becomes

$$-y^2 = \frac{3\left[R-\left(1-\frac{P}{N}\right)+\left(\frac{2AP}{N\sqrt{3}}\right)\right]^2}{\left(2R\left(1-\frac{P}{N}\right)\right)}\left(R\left(1-\frac{P}{N}\right)+\frac{AP}{\sqrt{3}N}-x\right) \tag{3}$$

Putting P= 1, 2, 3, …….. N-1 in equation (3) we will get the different parabola surfaces.

The die profile is considered at different depths with parameter (t=P/N) where the total die depth is assumed to be L. When t=0 i. e. at the entrance plane of die, z=0. When t=1, i.e. at the exit plane, z=OM=L

If the percentage reduction is (1-Q), then

$\frac{\pi R^2-\sqrt{3}A^2}{\pi R^2} = (1-Q)$ from where $A = R\sqrt{\left(\frac{\pi Q}{\sqrt{3}}\right)}$

For any value of 't' if y=0, then the coordinate of *O'* is $\left(R\left(1-t+\frac{t}{3}\sqrt{\pi Q}\right),0\right)$

Where $t = \frac{P}{N}$

The x co-ordinate of M and P is = $\left\{\left(\frac{R}{2}\right)\left(1-t+\frac{2t}{3}\sqrt{\pi Q}\right),\left(\frac{R\sqrt{3}}{2}\right)\left(1-t+\frac{2t}{3}\sqrt{\pi Q}\right)\right\}$ and $\left\{\left(\frac{R}{2}\right)\left(1-t+\frac{2t}{3}\sqrt{\pi Q}\right),-\left(\frac{R\sqrt{3}}{2}\right)\left(1-t+\frac{2t}{3}\sqrt{\pi Q}\right)\right\}$, respectively.

The equation of the parabola becomes

$$y^2 = 4\alpha\left(\left(R\left(1-t+\frac{t}{3}\left(\sqrt{\pi Q}\right)\right)-x\right)\right) \tag{4}$$

Substituting the coordinate of M into the parabola,

$$\left(\frac{3R^2}{4}\right)\left(1-t+\frac{2t}{3}\sqrt{\pi Q}\right)^2 = 4\alpha\left(R\left(1-t+\frac{t}{3}\sqrt{\pi Q}\right)-\left(\frac{R}{2}\right)\left(1-t+\frac{2t}{3}\sqrt{\pi Q}\right)\right)$$

α is determined to be

$$4\alpha = \frac{3R\left(1-t+\frac{2t}{3}\sqrt{\pi Q}\right)^2}{4\left(\frac{1}{2}-\frac{t}{2}-\frac{t}{3}\sqrt{\pi Q}\right)} \tag{5}$$

Putting the value of α in the equation (6.11), we get

$$y^2 = \frac{3R\left(1-t+\frac{2t}{3}\sqrt{\pi Q}\right)^2}{4\left(\frac{1}{2}-\frac{t}{2}-\frac{t}{3}\sqrt{\pi Q}\right)}\left(R\left(1-t+\frac{t}{3}\sqrt{\pi Q}\right)-x\right) \tag{6}$$

where $x = \frac{2A}{\sqrt{3}} = \frac{2}{\sqrt{3}}R\sqrt{\left(\frac{\pi Q}{\sqrt{3}}\right)}$ the distance of CG to any vertex of the triangle, t represents a depth parameter and the equation (6) gives the equation of the surface. This equation is called parametric equation where $t = z/L$, which then becomes the equation of the profile.

In a similar manner, the profiles of all the shapes considered were derived and tabulated below.

Geometry	Parametric equation	x
Square	$y^2 = \frac{R\left(1-t+t\sqrt{\pi\frac{Q}{2}}\right)}{\left(2\left(1-\frac{1}{\sqrt{2}}\right)(1-t)\right)}\left(R\left(1-t+t\sqrt{\pi\frac{Q}{4}}\right)-x\right)$	$x = \left(\frac{R}{2}\right)\sqrt{\pi Q}$
Triangle	$y^2 = \frac{3R\left(1-t+\frac{2t}{3}\sqrt{\pi Q}\right)^2}{4\left(\frac{1}{2}-\frac{t}{2}-\frac{t}{3}\sqrt{\pi Q}\right)}\left(R\left(1-t+\frac{t}{3}\sqrt{\pi Q}\right)-x\right)$	$x = \frac{2A}{\sqrt{3}} = \frac{2}{\sqrt{3}}R\sqrt{\left(\frac{\pi Q}{\sqrt{3}}\right)}$
Hexagonal	$y^2 = \frac{R\left(1-t+0.62t\sqrt{\pi Q}\right)^2}{\left(0.536(1-t)\right)}\left(R\left(1-t+0.31t\sqrt{\pi Q}\right)-x\right)$	$x = 2A = 0.62\sqrt{\pi Q}$
Heptagonal	$y^2 = \frac{0.188R\left(1-t+0.604t\sqrt{\pi Q}\right)^2}{\left(0.099(1-t)\right)}\left(R\left(1-t+0.31t\sqrt{\pi Q}\right)-x\right)$	$x = 2.305A = 0.604\sqrt{\pi Q}$
Octagonal	$y^2 = 4\alpha = \frac{0.854R\left(1-t+0.595t\sqrt{\pi Q}\right)^2}{\left(0.076(1-t)\right)}\left(R\left(1-t+0.298t\sqrt{\pi Q}\right)-x\right)$	$x = 2.305A = 0.604\sqrt{\pi Q}$

x = *the distance of CG to any vertex of the geometry*

Geometry of die profile for extrusion of H-, T- & L- Sections from round billet. If the percentage fraction of reduction is (1- Q), then

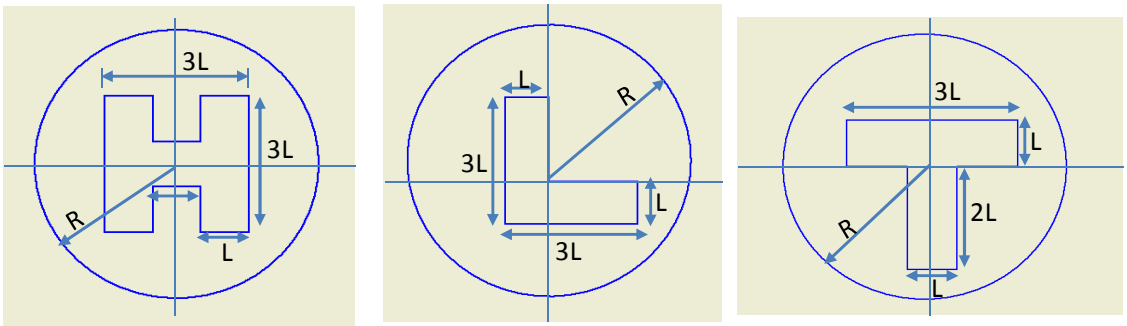

Fig. 2 The die profile (plan view) from round to H-, L- and T-sections

$\pi R^2 - 5l^2 = \pi R^2(1 - Q)$

where, $5l^2$ is the area of the square T and L- section

$5l^2 = \pi R^2 Q$

$l = R\sqrt{\frac{\pi Q}{5}}$

Therefore, l= the thickness of the square T-section

With the similar approach, H –section profile is derived to be $l = R\sqrt{\frac{\pi Q}{7}}$. Therefore, l= the thickness of the square H-section

Solid Model

MATLAB R2009b was used to generate the number of points using above generated die profile equation. The generated points were used to create solid model using Autodesk inventor 2013. Solid model generated from Autodesk inventor 2013 were show in the following figures 3-.8. FEM modeling has been carried out using 3D Deform software. A solid CAD model for the curved die profile is made using Autodesk Inventor. CAD model for extrusion of non- axisymmetric sections (T, L and H) from round billet are given in Fig. 3(a-c). The length of die is taken as 40mm. The solid CAD models are developed for 50% reduction.

Finite element simulation. The actual FEM-based analysis is carried out in this portion of DEFORM-3D. This simulation engine is based on a rigid-plastic FE formulation and can handle a multiple number of billets and dies with non-isothermal simulation capability. This is the programme which actually performs the numerical calculations for solution of the problem. In the present investigation, round billet of rigid plastic material for extrusion of triangular, square, hexagonal, heptagonal and octagonal section is modeled with a rigid curved die. The tetrahedral solid elements are taken for analysis. The work-material is taken as Aluminum AA6063, which is plastic in nature. The mesh is generated automatically. The constant friction factor is assumed in the modeling. The modeling has been carried out both for dry and lubricated condition. The values of 'm' are 0.38 and 0.75 for wet and dry conditions respectively. The operation has been carried out at simulation temperature of 30^{o}C.

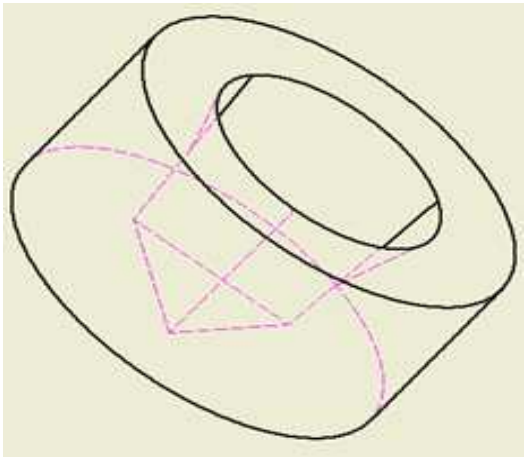

Fig. 3 Streamlined die for extrusion of square section from round billet

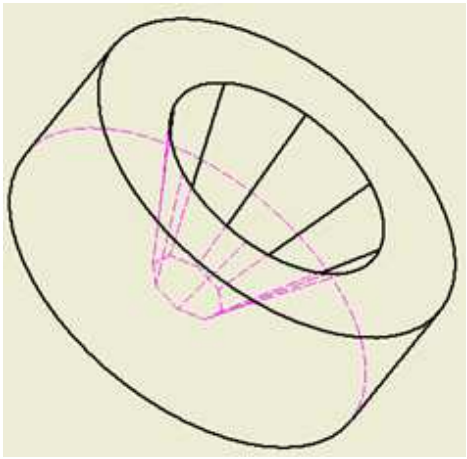

Fig. 4 Streamlined die for extrusion of heptagonal section from round billet

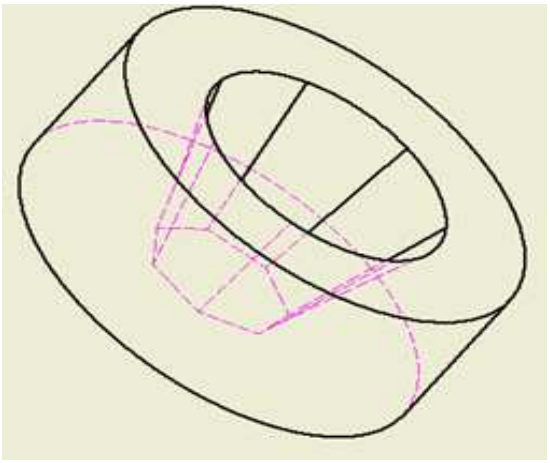

Fig. 5 Streamlined die for extrusion of octagonal section from round billet

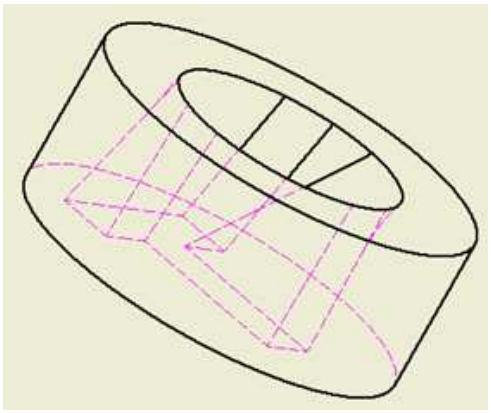

Fig. 6 Streamlined die for extrusion of T-section 50% Reduction

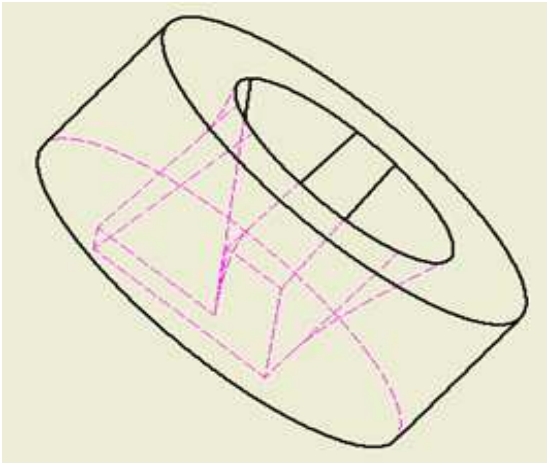

Fig. 7. Streamlined die for extrusion of L-section 50% Reduction

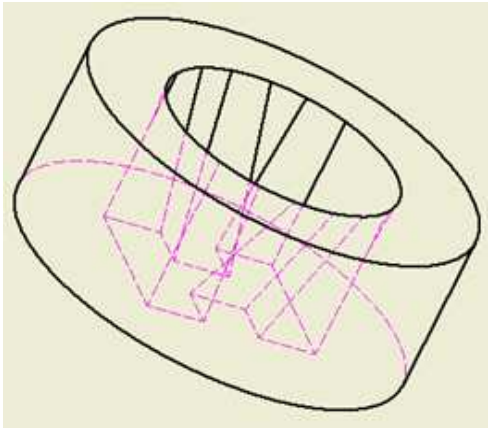

Fig. 8. Streamlined die for extrusion of H-section 50% Reduction

Results and Discussion

Extrusion load and punch displacement

.

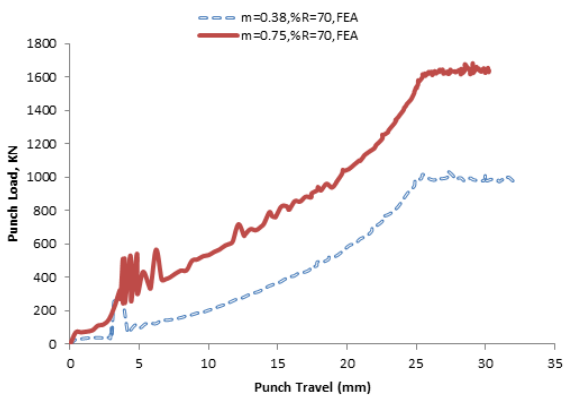

Fig. 9 Typical variation of punch load with punch travel for extrusion of circular from round section

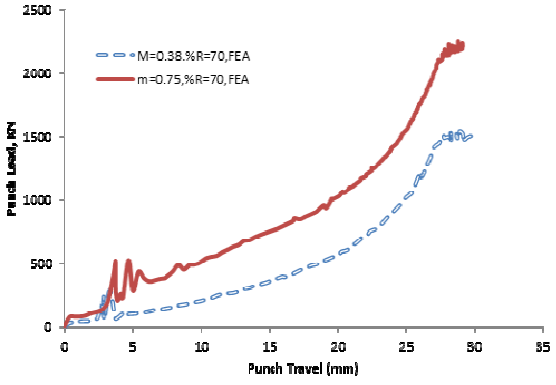

Fig. 10 Typical variation of punch load with respect to punch travel for extrusion of triangular section from round

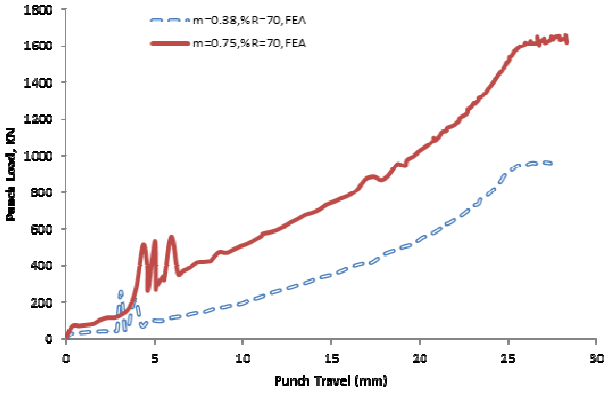

Fig. 11 Typical variation of punch load with respect to punch travel for extrusion of heptagonal section from round

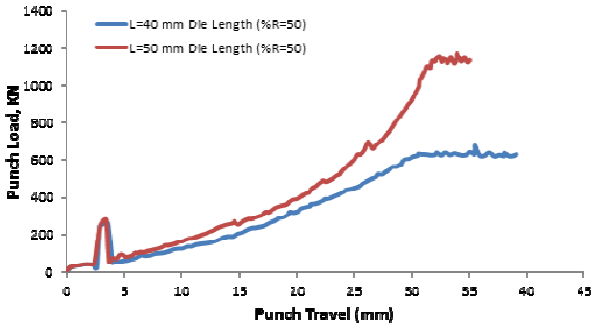

Fig. 12 Comparison of extrusion load versus punch travel of different die length

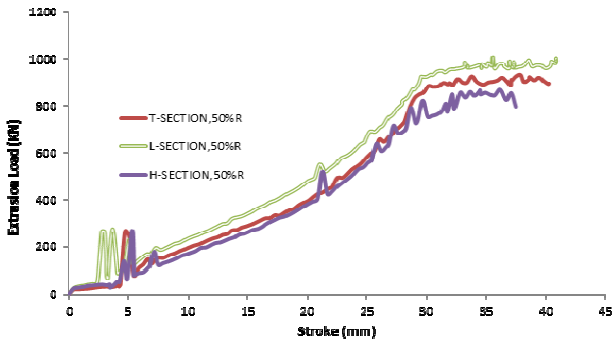

Fig. 13 Comparison of extrusion load versus punch travel of asymmetric geometry

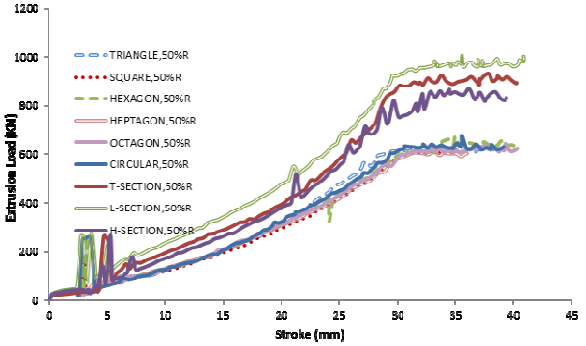

Fig. 14 Comparison of extrusion load versus punch travel for axisymmetric and symmetric geometry at 50%reduction

Figures 9 shows the plot of extrusion load against punch displacement during the extrusion of circular cross-section from round billet at percentage area reductions of 70 for wet (friction factor, m = 0.38) and dry (friction factor, m = 0.75) conditions. The effect of friction factor is succinctly seen from the two plots as the dry condition shows higher extrusion load than the wet condition. The kink or wavy observation at the stage of filling of the container is more pronounced at higher friction or dry condition. For figure 10, representing the extrusion of triangular section from circular billets at the same conditions stated above for circular section, the effect of friction factor is again more pronounced in the dry condition showing higher extrusion load than the wet condition. The kink or wavy observation at the stage of filling of the container is more pronounced at higher friction or dry condition. Also, comparing the two plots, the higher percentage reduction shows the higher extrusion load. However, plots representing friction of m = 0.75, shows no distinct maximum extrusion load like that of m = 0.38. This is probably due to adverse friction condition within the extrusion chamber. This is likely to adversely affect the structure of the extrudate. Figure 11shows the extrusion load versus punch displacement in the extrusion of heptagonal section from round billet. The observation here looks similar to circular section from round billet (figures 9). This shows that friction effect is still more pronounced in the extrusion of heptagonal section than in circular section. Figure 12 shows the punch or extrusion load versus punch travel at different die length. It is seen that the higher die length gives the higher extrusion load. This is probably due to the frictional power accruing from additional length. A comparison of extrusion loads versus punch displacements or stroke curves for the aluminium alloy AA6063 is shown in Fig. 13 for extrusion of H, T and L-section from round billet through curve dies for 50% reduction. It is found that the extrusion pressure is highest for L-section followed by T-section while that of H-section gives the least. The similar comparison of extrusion loads versus punch displacements or stroke curves for the aluminium alloy AA6063 is shown in Fig. 14 for extrusion of axisymmetric (circular, triangular,

square, hexagonal, heptagonal and octagonal) shaped sections and non-axisymmetric (T, L and H) shaped sections from round billet through curve dies for 50% reduction at room temperature. While there is no marked difference between the predictive load for symmetric shapes, the L-section has the highest extrusion load, followed by T-section and the H-section given the least pressure for asymmetric extrusion.

Table 1. Maximum dimensionless extrusion pressure of various geometries and at indicated percentage area reductions

Geometry		**Wet (m = 0.38)** $\frac{P}{\sigma_o}$			**Dry(m = 0.75)** $\frac{P}{\sigma_o}$			**r = 90% (m = 0.38)**
	r=50%	***r=50% Exper.***	***r=70%***	***Max. temp (°C)***	***r=50%***	***r=70%***	***r=90%***	***Max. temp (°C)***
Triangle	1.68		2.37	44.4	2.68	3.86	5.55	44.4
Square	1.51	1.48[16]	2.18	41.1	2.66	3.68	5.38	41.1
Hexagonal	1.39		2.12	40.0	2.45	3.43	5.04	40.0
Heptagonal	1.30		2.12	40.2	2.43	3.40	5.11	40.2
Octagonal	1.28		2.01	40.6	2.43	3.45	5.14	40.6
Circular	1.31		2.12	40.6	2.11	3.39	5.06	40.6
H-section	1.80							
T-section	1.92							
L-section	2.03							

Table 1 shows the maximum dimensionless extrusion pressure and temperature of various geometries at indicated percentage area reductions. Generally, it can be observed that as the side of the considered polygons increases, the extrusion pressure decreases for both wet and dry conditions at the indicated percentage area reductions. This is probably due to the ease of metal flow as the shape of exit geometry is approaching the shape of entry geometry and moreover the die cross section is designed to gradually reduce from circular to the exit polygon. The maximum temperature generated also follows the same pattern with triangular given the highest temperature, followed by square while the remaining geometries, such as hexagonal, heptagonal, octagonal and circular virtually maintained the same temperature. The load prediction versus punch travel are shown in figures 29-32 for extrusion of T, L, H and circular sections from round billet for 50% reduction for lubricated condition (m=0.38), respectively. The extrusion load as it is felt by all the components, such as the billet, container, bottom die and the punch, involved is shown below in figures 29-31. Notice that in all the three graphs, the billet resists load least, followed by the container and then the bottom die while the punch felt the load most during the operation. Also, while the wavy behaviour was rather more pronounced with the container and the punch, it's almost not seen at in the billet deformation as well as in the bottom die. This wavy behaviour is probably due to the initial filling of the die by the billet as it is seen to be more pronounced as the complexity of the die increases. This is corroborated in figure 32 below which depicts the extrusion of circular shape from circular billet. The wavy observation is practically nonexistence in this case when compared with L-, T- and H-sections. This observation is logical since it is easier to convert gradually, which the method is adopted in this paper, from round billet to round shape. This wavy observation is likely to impact on the live span of the tools.

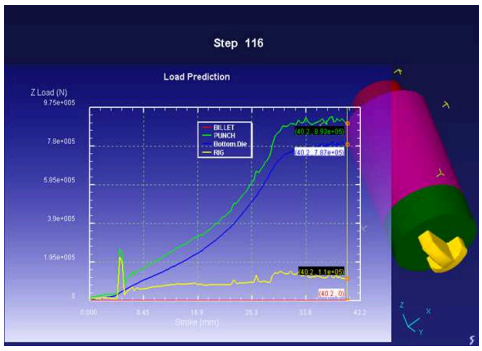

Fig. 15 Variation of punch load with respect to punch travel for extrusion of T- section m=0.38 (50% reduction)

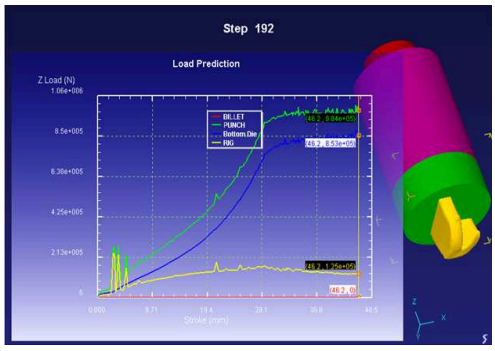

Fig. 16 Variation of punch load with respect to punch travel for extrusion of L- section m=0.38 (50% reduction)

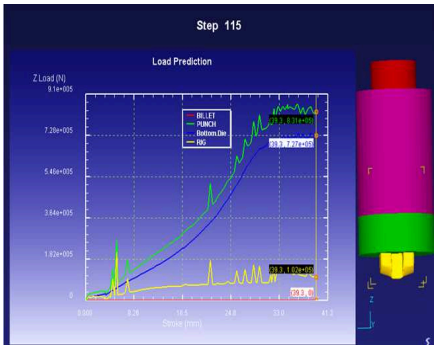

Fig. 17 Variation of punch load with respect to punch travel for extrusion of H- section m=0.38 (50% reduction)

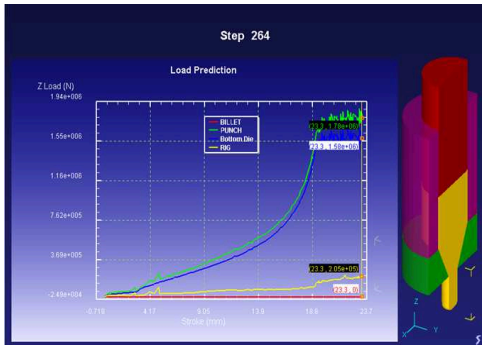

Fig. 18 Variation of punch load with respect to punch travel for extrusion of circular section

Conclusion

Finite element simulation has been successfully carried out for symmetric and asymmetric shapes. It is found that the predictive loads for asymmetric shapes are found to be higher than that of the symmetric shapes. While there is no marked difference between the predictive loads for symmetric shapes that of the asymmetric shapes is significant where L-section has the highest extrusion load, followed by T-section and the H-section given the least pressure. A comparison between the available experimental data and the numerical results of the simulation shows good agreement.

References

[1] T. Sheppard, *Extrusion of AA2024 Alloy*, Materials Science Technology 9 (1993) 430-440.

[2] N. Solomon and I. Solomon, *Effect of die shape on the metal flow pattern during direct extrusion process*, Revista de Metalurgia, 46 (5), 2010, 396-404

[3] I. Flitta, T. Sheppard and Z. Peng, *FEM analysis to predict development of structure during extrusion and subsequent solution soak cycle,* Materials Science and Technology, 23 (5) 2007, 582-592

[4] *Libura*, *W.*& *Zasadzinski*, *J.*, "*The influence of strain gradient on material structure during extrusion of the AlCu4Mg alloy"*, Journal of Material Processing Technology, vol. *34*, *1992*, p.*517*-524

[5] M. Jolgaf, S.B. Sulaiman, M.K.A. Ariffin, and A.A. Faieza, *Billet Shape Optimization for Minimum Forging Load* , European Journal of Scientific Research, 24 (3) (2008), 420-427

[6] R. Narayanasamy, R. Ponalagusamy, R. Venkatesan, P. Srinivasan, *An upper boundary solution to extrusion of circular billet to circular shape through cosine dies*, Materials and Design 27 (2006) 411–415

[7] W.A. Gordon, C.J. Van Tyne, Y.H. Moon, *Overview of adaptable die design for extrusions*, Journal of Materials Processing Technology 187–188 (2007) 662–667

[12] K. P. Maity, A. K. Rout, Kalu Majhi, *computer-aided simulation of metal flow through curved die for extrusion of square section from square billet* , Presented in International Conference on Extrusion and Benchmark, Dortmund, Germany, 16-17 September, 2009

[14] T. Chanda, J. Zhou, J. Duszczyk, *FEM analysis of aluminium extrusion through square and round dies* , Materials and Design 21 (2000) 323-335

[15] Zhi Peng, Terry Sheppard, *Simulation of multi-hole die extrusion,* Materials Science and Engineering A 367 (2004) 329–342

[16] OO. Onawola and MB. Adeyemi, *Warm compression and extrusion tests of Aluminium*, Journal of Materials Processing Technology, 2005, 136, 7-11

Metal Forming 2014
10.4028/www.scientific.net/KEM.622-623

Load Prediction for the Extrusion from Circular Billet to Symmetric and Asymmetric Polygons Using Linearly Converging Die Profiles

10.4028/www.scientific.net/KEM.622-623.119

DOI References

[1] T. Sheppard, Extrusion of AA2024 Alloy, Materials Science Technology 9 (1993) 430-440.
http://dx.doi.org/10.1179/mst.1993.9.5.430
[6] R. Narayanasamy, R. Ponalagusamy, R. Venkatesan, P. Srinivasan, An upper boundary solution to extrusion of circular billet to circular shape through cosine dies, Materials and Design 27 (2006) 411-415.
http://dx.doi.org/10.1016/j.matdes.2004.11.026
[7] W.A. Gordon, C.J. Van Tyne, Y.H. Moon, Overview of adaptable die design for extrusions, Journal of Materials Processing Technology 187-188 (2007) 662-667.
http://dx.doi.org/10.1016/j.jmatprotec.2006.11.158
[14] T. Chanda, J. Zhou, J. Duszczyk, FEM analysis of aluminium extrusion through square and round dies , Materials and Design 21 (2000) 323-335.
http://dx.doi.org/10.1016/S0261-3069(99)00073-4
[15] Zhi Peng, Terry Sheppard, Simulation of multi-hole die extrusion, Materials Science and Engineering A 367 (2004) 329-342.
http://dx.doi.org/10.1016/j.msea.2003.10.294